Indian J. Phys. **78 (6)**, 495-504 (2004)

INTERNATIONAL JOURNAL
IJP

Particle aspect analysis of the electrostatic ion-cyclotron instability : effects of ion and electron beam and general distribution function

Ruchi Mishra and M S Tiwari*
Department of Physics & Electronics, Dr. H S Gour Viswavidyalaya, Sagar-470 003, Madhya Pradesh, India
E-mail : tiwarims@yahoo.co.in

Received 3 September 2003, accepted 20 April 2004

Abstract : Dispersion relation, resonant energy transferred, growth rate and marginal stability of the electrostatic ion cyclotron wave (with general loss-cone distribution function in low β homogeneous plasma) in the presence of upgoing ion beam and downcoming electron beam are discussed by investigating the trajectories of the charged particles The wave is assumed to propagate obliquely to the static magnetic field. The whole plasma is considered to consist of resonant and non-resonant particles. It is assumed that resonant particles participate in energy exchange with the wave whereas non-resonant particles support the oscillatory motion of the wave. Effects of the steepness of the loss-cone distribution and ion and electron beam velocities on resonant energy transferred and growth rate of the instability are discussed. It is found that the effect of upgoing ion beam is to stabilize the wave and enhance the transverse acceleration of ions whereas the downcoming electron beam acts as a source of free energy for the electrostatic ion-cyclotron wave and enhances the growth rate. Effect of steepness of loss cone is also to enhance the growth rate and decrease the transverse acceleration of ions. The results are interpreted for the space plasma parameters appropriate to the auroral acceleration region.

Keywords : Electrostatic ion cyclotron wave, auroral acceleration region, loss-cone, ion and electron beam.

PACS Nos. : 52.35.Hr, 52.35.Qz, 94.10.Rk

1. Introduction

The electrostatic ion-cyclotron (EIC) instability has been of considerable interest to plasma physicists since the instability appears in almost all types of magnetized plasma and under a variety of physical conditions ranging from fusion and laboratory experiments to space plasma. The EIC waves are of great importance in the auroral topside ionosphere as these waves can be excited for a wide range of ionospheric parameters [1]. These waves are one of the most important plasma wave modes in the near-earth space plasma environment as well. The EIC wave requires a smaller value of magnetic field aligned current to be unstable [1], can act as an ion heating source [2] and provide anomalous resistivity [3]. Because of these properties, it has been invoked in explanation of various phenomena observed in earth's auroral acceleration region *e.g.* observation of wave activity in the ion cyclotron range of frequencies, strong transverse heating of heavy ions [2], ion-conic formation [4], generation of broad band extremely low frequency waves [5] and ion-acoustic like waves [6], inverted-V structures in magnetosphere-ionosphere coupling [7,8] and various effects.

Plasma wave measurements from S3-3 satellite, sounding rocket, backscatter radar have observed EIC waves at a broad range of altitudes, which include low altitude ionosphere (300–600 km) [9], topside ionosphere (~900 km) [4] and higher altitudes (2600 km). Recently, a polar satellite traversing the northern auroral region at altitudes of about 30000 km, has observed EIC waves in the perpendicular field [10]. The same satellite has also observed local EIC waves in a region containing perpendicularly heated ion distribution, in the auroral zone, in the magnetosphere and at lower altitudes. Recent

*Corresponding Author

observations by the FAST satellite also indicate existence of EIC waves in the upward current auroral region [11].

Ion and electron beams have been observed over a wide region associated with the whole auroral oval. Over the last decade, it has been established that auroral luminosity is due to the impact of an accelerated electron beam coming towards the ionosphere and at the same event, an ion beam moving towards the magnetotail [12]. Laboratory experiments on EIC turbulences showed that ion heating results in a low-density warm core surrounded by a denser hot ion cloud. Therefore, high-level ion-cyclotron turbulence can be sustained in a core of ion gyro-radius scale. Thus, it is possible for an unstable field aligned current to produce fine structures in an unstable field aligned region and lead to the formation of auroral arcs embedded in the inverted-V precipitation region.

The parallel potential drop along the auroral field lines may lead to the downcoming electrons and up-flowing ion beams. Plasma wave measurements from the various satellites like Hawkeye-1, Imp-6, DE-1, DE-2, Viking *etc* show that a broad region of intense plasma wave turbulence occurs in the region of the field aligned current on high latitude auroral field lines at altitudes above few thousand kilometers during the periods of substorm activity [13]. Observations have shown the presence of ion and electron beams in the plasma sheet boundary layer [14]. Recent observations by the Polar satellite also indicate upgoing ion beams and downcoming accelerated electrons in the low altitude boundary and high altitude of auroral acceleration region [15].

Recently, Mozer and Hull [15] have studied upgoing ion beams and downcoming electron beams in the low altitude boundary and high altitude of auroral acceleration region using the data obtained from a Polar satellite. In the present work, we have utilized their data to study the interaction of ion and electron beams with EIC waves and hence the auroral acceleration phenomena.

Collisional effects on the EIC instability in a dusty plasma have been carried out by Bharuthram *et al* [16]. Simulations of ion-cyclotron mode in magnetoplasma with transverse inhomogeneous electric field for Maxwellian plasma have been carried by Ganguli [2]. Gavrishchaka *et al* [17] studied the EIC mode in a two ion component plasma with transverse velocity shear. The behaviour of multicomponent anisotropic plasma in a magnetic flux tube in the presence of current driven EIC turbulence is studied by Zakhrov and Meister [18].

In most of the theoretical work reported so far, the velocity distribution functions have been assumed to be either ideal Maxwellian or bi-Maxwellian [2,16–18], ignoring the steep loss-cone feature. Plasma in mirror like devices and in the auroral region with curved and converging field lines, considerably depart from Maxwellian distribution, and have steep loss-cone distribution [19]. In the present work, for the first time, the general distribution function is used to study the EIC waves in the presence of ion and electron beam. The present analysis is based on Dawson's theory [20] of Landau damping, which has been further extended by Terashima [21].

In the present work, the particle aspect analysis of the EIC wave has been studied by incorporating the details of particle trajectories in the presence of upgoing ion beams and downcoming electron beams and the general distribution function. The advantage of this approach is its suitability for dealing with auroral electrodynamics involving the current system, acceleration and energy exchange by wave-particle resonant interaction. The method is more accurate than the MHD approach in dealing with finite gyro-radius effects and temperature anisotropies.

2. Basic assumptions

The basic assumptions are the same as in earlier work by Terashima [21]. The plasma is considered to be homogeneous and collisionless consisting of resonant and non-resonant particles. The ions are supposed to have unit charge. The wave is considered to be propagating obliquely to the static uniform magnetic field $\boldsymbol{B}_0$ that is along the z-direction. The non-resonant particles support the oscillatory motion of the EIC wave while the resonant particles participate in energy exchange with the wave. An EIC wave is assumed to start at $t = 0$ when the resonant particles are not disturbed. The trajectories of particles are then evaluated within the framework of linear theory. Using the particle trajectory in the presence of EIC wave, the dispersion relation and the growth rate is derived for different distribution indices.

The wave is assumed to have the form

$$k \| E,\ k = (k_\perp, 0, k_\parallel),\ E = (E_x, 0, E_z)$$

with

$$E_x(r,t) = E_1 \cos((k_\perp x + k_\parallel z - \omega t),$$
$$E_z(r,t) = \kappa E_1 \cos((k_\perp x + k_\parallel z - \omega t), \quad (1)$$

$$\kappa = \left(\frac{k_\parallel}{k_\perp}\right) < 1.$$

The amplitude E_1 is a slowly varying function of t *i.e.*

$$\frac{1}{E_1}\left(\frac{dE_1}{dt}\right) << \omega .$$

In the present analysis, the EIC instability in the system of hot electrons and hot ions is considered under the condition [21]

$$\omega \sim \ell \Omega_i,$$

$$V_{T\|i} < \left|\frac{\omega - \ell\Omega_i}{k_\parallel}\right| << V_{T\|e},$$

$$1 > \kappa^2 \cong \frac{k_\parallel^2}{k_\perp^2}\left(\frac{\omega - \ell\Omega_i}{\Omega_i}\right)^2$$

and

$$k_\perp^2 \rho e^2 << k_\perp^2 \rho_i^2 \sim 1, \quad (2)$$

where $V_{T\|i,e}$ is the thermal velocities of the ions and electrons respectively along the magnetic field, Ω_i is the gyro-frequency of the ion $\ell = 1, 2, \ldots\ldots$ represents the harmonics of the wave, $\rho_{i,e}$ is the mean gyro-radii of the ions and electrons respectively ω represents the wave frequency, $k_\parallel$ and $k_\perp$ are the components of the wave vector along and across the magnetic field respectively.

3. Particle trajectories and velocities

In the present mathematical analysis the procedure adopted by Terashima [21] is followed. The equation of motion of a particle is given by

$$m\left(\frac{dv}{dt}\right) = q\left[E + \left(\frac{1}{c}\right) v \times B_0\right], \quad (3)$$

where symbols have their usual meaning.

If E is considered to be a small perturbation, velocity v can be expressed in terms of unperturbed velocity V and perturbed velocity u. The perturbed velocity u is determined by

$$\frac{du_\parallel}{dt} = \frac{q\kappa E_1}{m}\sum_{-\infty}^{+\infty} J_n(\mu)\cos\left(\Lambda_n t + \Psi_n^0\right),$$

$$\frac{du_\perp}{dt} + i\Omega u_\perp = \frac{qE_1}{m}\sum^{+\infty} J_n(\mu)\cos\left(\Lambda_n t + \Psi_n^0\right), \quad (4)$$

where $u_\perp = u_x + iu_y$ represents the perturbed velocity in transverse direction and $u_\parallel$ represents the perturbed velocity in parallel direction. The basic trajectories are the same as derived by Terashima [21]. The resonance criteria is given by

$$\Lambda_n(V_\parallel = V_r) = k_\parallel V_r - \omega + \ell\Omega_i = 0;\ \ell = \pm 1, \pm 2, \ldots\ldots, \quad (5)$$

where V_r is the resonance velocity of the particles and the particles with parallel unperturbed velocity '$V_\parallel$' near to $V_r = \frac{\omega - \ell\Omega_i}{k_\parallel}$ are the resonant particles which in this case, are the ions. This resonance condition means that for ions, the wave appear to be independent of 't' in the particles frame, $J_n(\mu)$ and $J_\ell(\mu)$ are Bessel's functions which arise from the different periodical variations of charged particles trajectories and $\mu = \frac{k_\perp V_\perp}{\Omega_i}$. The term represented by the Bessel's function indicates the reduction in the field intensity due to finite gyro-radius effect. The oscillatory solution of $u(t)$ is given by

$$u_x(r,t) = \frac{qE_1}{m}\sum^{+\infty} J_n(\mu)\sum^{+\infty} J_\ell(\mu)\left[\frac{\Lambda_n}{\Lambda_n^2 - \Omega_i^2}\sin\chi_{n\ell}\right.$$
$$\left. - \frac{\delta}{2\Lambda_{n+1}}\sin(\chi_{n\ell} - 2\Lambda_{n+1}t) - \frac{\delta}{2\Lambda_{n-1}}\sin(\chi_{n\ell} - 2\Lambda_{n-1}t)\right],$$

$$u_y(r,t) = \frac{qE_1}{m}\sum^{+\infty} J_n(\mu)\sum^{+\infty} J_\ell(\mu)\left[\frac{\Omega_i}{\Lambda_n^2 - \Omega_i^2}\cos\chi_{n\ell}\right.$$
$$\left. \frac{\delta}{2\Lambda_{n+1}}\cos(\chi_{n\ell} - 2\Lambda_{n+1}t) - \frac{\delta}{2\Lambda_{n-1}}\cos(\chi_{n\ell} - 2\Lambda_{n-1}t)\right],$$

$$u_z(r,t) = \frac{qKE_1}{m}\sum_{-\infty}^{+\infty} J_n(\mu)\sum_{-\infty}^{+\infty} J_\ell(\mu)\frac{1}{\Lambda_n}$$

$$[\sin\chi_{n\ell} - \delta\sin(\chi_{n\ell} - \Lambda_n t)], \tag{6}$$

where $\chi_{n\ell} = \boldsymbol{k}\cdot\boldsymbol{r} - \omega t + (n-\ell)(\Omega_i t - \theta)$, (7)

$\delta = 0$ for non-resonant particles and $\delta = 1$ for resonant particles.

4. Density perturbation

To find out density perturbation associated with the velocity perturbation $u(r,t)$ we consider the eq.

$$\frac{dn_1}{dt} = -N(V)(\nabla.u). \tag{8}$$

Expressing the R.H.S. of eq. (8) as the function of t and the initial parameters and integrating eq. (8), we get $n_1(r,t)$, the perturbed density for the non-resonant and resonant particles as

$$n_1(r,t) = \frac{qE_1N}{m}\sum_{-\infty}^{+\infty} J_n(\mu)\sum_{-\infty}^{+\infty} J_\ell(\mu)$$

$$\left[\frac{\Lambda_n^2}{\Lambda_n^2 - \Omega_i^2} + \frac{\kappa^2 k_\perp}{\Lambda_n^2}\right]\sin\chi_{n\ell}, \tag{9}$$

$$n_1(r,t) = -\frac{qE_1N\kappa^2k_\perp}{m}\sum_{-\infty}^{+\infty} J_n(\mu)\sum_{-\infty}^{+\infty} J_\ell(\mu)\frac{1}{\Lambda_n^2}$$

$$[\sin\chi_{n\ell} - \sin(\chi_{n\ell} - \Lambda_n t) - \Lambda_n t\cos(\chi_{n\ell} - \Lambda_n t)] \tag{10}$$

provided that $\omega \sim \ell\Omega_i$

and

$$\kappa^2 = \left(\frac{k_\parallel}{k_\perp}\right)^2\left\langle\left|\frac{\Lambda_n^2}{\Lambda_n^2 - \Omega_i^2}\right|\right\rangle \approx \frac{\Lambda_n^2}{\Omega_i^2}. \tag{11}$$

5. General distribution function

To calculate the dispersion relation and growth rate, the general loss-cone distribution function of the following form [19] is used

$$N(y,V) = N_0\left\{1 - \varepsilon\left(y + \frac{V_x}{\Omega_i}\right)\right\}f_\perp(V_\perp)f_\parallel(V_\parallel), \tag{12}$$

$$f_\perp(V_\perp) = \frac{V_\perp^{2J}}{\pi V_{T\perp}^{2(J+1)}J!}\exp\left\{-\frac{V_\perp^2}{V_{T\perp}^2}\right\}$$

and $f_\parallel(V_\parallel)$ is defined by the drifting Maxwellian

$$f_\parallel(V_\parallel) = \frac{1}{\sqrt{\pi}V_{T\parallel}}\exp\left\{-\frac{(V_\parallel - V_{Dj})^2}{V_{T\parallel}^2}\right\}, \tag{13}$$

where N_0 is the background plasma density, ε is a small parameter of the order of inverse of 'density gradient scale length', $J = 0, 1, 2,.....$ is the distribution index, also known as the steepness of the loss-cone. For $J = 0$, this distribution represents a bi-Maxwellian distribution and for $J = \infty$, this reduces to Dirac-Delta function. $V_{T\parallel}^2 = (J+1)^{-1}(2T_\perp/m)$ are the squares of parallel and transverse thermal velocities with respect to the external magnetic field. Index 'J' characterizes the width of the loss-cone. Moreover, $f_\perp(V_\perp)$ is peaked about $J^{1/2}V_{T\perp}$ and has a half width of $\Delta V_\perp \sim J^{-1/2}/V_{T\perp}$. V_{Dj} defines the beam velocity of the particles and subscript j stands either for electrons or ions.

6. Dispersion relation

Applying the charge neutrality condition $\tilde{n}_i \approx \tilde{n}_e$, where $\tilde{n}_{i,e}$ are the integrated perturbed densities for the non-resonant particles, and using eqs. (9) and (12), we obtain

$$n_e \equiv \left|\frac{1}{k_\perp d_{\parallel e}^2}\right|\frac{E_1}{4\pi e}\sin(\boldsymbol{k}\cdot\boldsymbol{r} - \omega t), \tag{14}$$

$$\tilde{n}_i \equiv -\frac{k_\perp\kappa^2\omega_{pi}^2}{[(\omega - k_\parallel V_{Di}) - \ell\Omega_i]^2}\left\langle J_\ell^2\right\rangle\frac{E_1}{4\pi e}\sin(\boldsymbol{k}\cdot\boldsymbol{r} - \omega t), \tag{15}$$

where $\omega_{pi,e}^2 = \dfrac{4\pi n_0 e^2}{m_i}$

and $\left\langle J_\ell^2\right\rangle = \int 2\pi V_\perp dV_\perp J_\ell^2(\mu)f_{\perp i}(V_\perp)$

$$= \exp\left(-\frac{k_\perp^2\rho_i^2}{2}\right)I_\ell\left(\frac{k_\perp^2\rho_i^2}{} \right. \tag{16}$$

where $I_\ell\left(\frac{k_\perp^2\rho_i^2}{}\right)$ is modified Bessel function.

The Debye length '$d_{\|e}$' corresponding to mean parallel energy is given by

$$d_{\|e}^2 = \frac{T_{\|e}}{m_e\omega_{pe}^2} \tag{17}$$

Using the Poisson's equation

$$\nabla.E = -k_\perp(1+\kappa^2)E_1\sin(kx-\omega t) = 4\pi(\tilde{n}_i - \tilde{n}_e) \tag{18}$$

and perturbed ion and electron density $\tilde{n}_i$ and $\tilde{n}_e$, the dispersion relation is obtained as

$$1+\frac{1}{1+\kappa^2}\left\|\frac{1}{\kappa_\perp^2 d_{\|e}^2}\right.\left(\frac{\omega^2}{1+\kappa^2}\right.$$

$$\left.\frac{\omega_{pi}^2}{\{(\omega-k_\| V_{Di})-\ell\Omega_i\}^2}\right]\left\langle\left(J_{\ell+1}^2+J_{\ell-1}^2\right)\right\rangle \equiv 0\,. \tag{19}$$

$$\ell=1, <(J_0^2+J_2^2)> = 1-(J+1)b_i;\ <(J_0+J_2)^2>$$

$$= 1-\frac{1}{2}(J+1)b_i; b_i = \frac{k_\perp^2\rho_i^2}{2}\,. \tag{20}$$

For $J = 0$ and $V_{Di} = 0$, this despersion relation reduces to that given by Terashima [21].

7. Calculation of energy and growth rate

The wave energy density 'W_W' per unit wavelength is the sum of pure field energy and the changes in the energy of the non-resonant particles *i.e.* $W_W = \frac{\lambda W_1^2}{8\pi} + W_e + W_i$, which comes out to be

$$W_W = \frac{\lambda W_1^2}{8\pi} + \frac{\lambda E_1^2}{16\pi}\frac{\omega_{pi}}{\{(\omega-k_\| V_{Di})-\ell\Omega_i\}^2}$$

$$\times\kappa^2\,{}^1\left\langle J_{\ell-1}^2+J_{\ell+1}^2\right\rangle + \frac{\lambda E_1^2}{16\pi}\left(\frac{1}{k_\perp^2 d_{\|e}^2}\right), \tag{21}$$

where

$$\frac{\left\langle\left(J_{\ell-1}+J_{\ell+1}\right)^2\right\rangle}{\left\langle J_{\ell-1}^2+J_{\ell+1}^2\right\rangle}\,. \tag{22}$$

Here, the ions contribution is dominant unless $k_\perp^2 d_{\|e}^2 < 1$.

The transverse energy and parallel energy of the resonant ions are calculated to be

$$W_{r\perp} = \left(\frac{\lambda E_1^2}{8}\right)\left(\frac{\omega_{pi}^2}{\Omega_i^2}\right)\left(\frac{\omega_i}{k_\| V_{\text{thi}}}\right)\frac{\Omega_i t}{\sqrt{2\pi}}$$

$$\times\exp\left[-\frac{1}{2}\left(\frac{\omega_i}{k_\| V_{\text{thi}}}\right)^2\left(1-\frac{\ell\Omega_i}{\omega_i}\right)^2\right.$$

$$\times\frac{1}{2}\left\langle J_{\ell-1}^2+J_{\ell+1}^2\right.\left.1-\frac{R\left(\frac{\ell-\Omega_i}{\omega}-\right.}{\frac{\ell\Omega_i}{\omega_i}}\right.\frac{T_{\perp i}}{T_{\|i}} \tag{23}$$

$$W_{r\|} = \left(\frac{\lambda E_1^2}{8}\right)\left(\frac{\omega_{pi}^2}{\Omega_i^2}\right)\left(\frac{\omega_i}{k_\| V_{\text{thi}}}\right)\frac{\Omega_i t}{\sqrt{2\pi}}$$

$$\times\exp\left\{-\frac{1}{2}\left(\frac{\omega_i}{k_\| V_{\text{thi}}}\right)^2\left(1-\frac{\ell\Omega_i}{\omega_i}\right.\right.$$

$$\times\frac{1}{2}\left\langle\left(J_{\ell-1}+J_{\ell+1}\right)^2\right.\left.\frac{1-\frac{\ell\Omega_i}{\omega_i}}{\frac{\ell\Omega_i}{\omega_i}}\right.\frac{T_{\perp i}}{T_{\|i}}\,, \tag{24}$$

where $\omega_i = \omega - k_\| V_{Di}$.

Using the law of conservation of energy

$$\frac{d}{dt}(W_W + W_r) = 0\,. \tag{25}$$

The growth rate is derived as

$$\gamma = \frac{1}{E_1}\left(\frac{dE_1}{dt}\right) = -\frac{dW_r}{dt}\Big/2W_W\,. \tag{26}$$

Also $\left|\frac{dW_{r\perp}^i}{dt}\right. >> \frac{dW_{r\|}^i}{dt}$ (27)

Hence, the growth rate defined in eq. (26) is given by

$$\frac{\gamma}{\omega} = \sqrt{\frac{\pi}{2}}\left(\frac{\omega_i}{k_\parallel V_{thi}}\right)\left(1-\frac{\ell\Omega_i}{\omega_i}\right)^2$$

$$\times \exp\left\{-\frac{1}{2}\left(\frac{\omega_i}{k_\parallel V_{thi}}\right)^2\left(1-\frac{\ell\Omega_i}{\omega_i}\right)^2\right\}\left[R\left(\frac{\left(\frac{\ell\Omega_i}{\omega_i}-1\right)}{\frac{\ell\Omega_i}{\omega_i}}\right)\frac{T_{\perp i}}{T_{\parallel i}}-1\right], \quad (28)$$

where ℓ = 1, 2, 3..... is to be substituted and R is given eq. (22). Here it is to noted that J and the beam affects the growth rate. For J = 0 and V_{Di} = 0, the result is the same as derived by Terashima [21].

8. Marginal instability

For the marginal unstable condition $\gamma = 0$, we then arrive at the result

$$V_{Di} = \frac{\ell\Omega_i}{k_\parallel}\left[1-\left(\frac{T_{\parallel i}}{T_{\perp i}R}\right)\right]-\frac{\omega}{k_\parallel} \quad (29)$$

which shows that ion beam may be a source of EIC wave generation besides the temperature anisotropy and the steep loss-cone. When both $T_{\perp i}/T_{\parallel i}$ and R are greater than unity and $\omega < \Omega_i$ wave generation by ion beam is possible. For the plasma parameters mentioned in the result and discussion and ω = 309 s^{-1}, the estimated value of V_{Di} for the wave generation in the auroral acceleration region is of the order of 10^6 m/s which is in accordance with the observations on the auroral field lines [15].

9. Results and discussion

In the present analysis, the expressions for the dispersion relation, resonant energies and growth rate are derived in the presence of an upgoing ion beam, downcoming electron beam and the steepness of the loss-cone index. The following parameters relevant to the auroral acceleration region [10,15] are used to evaluate the dispersion relation, resonant energies, and growth rate :

B_0 = 4300 nT at 1.4 R_E, Ω_i = 412 s^{-1}, ℓ = 1, λ = 300 m, $E_\perp$ = 50 mV/m, ω_{pi}^2/Ω_i^2 = 2, b_i = 0.1, $k_\parallel$ = 0.00002 m^{-1}, $T_\perp/T_{\parallel i}$ = 50 and $\Omega_i t$ = 10.

The effect of ion beam velocity (V_{Di}) and distribution index (J) on the growth rate and the resonant energies transferred, is depiced in Figures 1, 2 and 3. Figure 1 depicts the variation of growth rate (γ/ω) with that wave

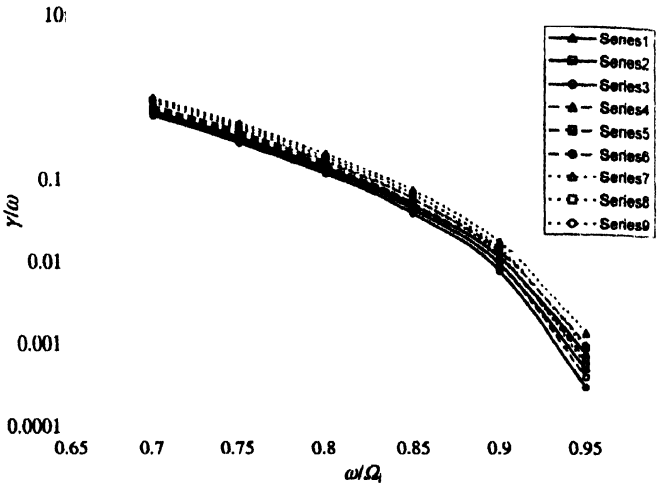

Figure 1. Variation of γ/ω with ω/Ω_i for different values of V_{Di} and J. [Series-1 : J = 0, V_{Di} = – 100000 m/s; Series-2 : J = 0, V_{Di} = – 200000 m/s; Series-3 : J = 0, V_{Di} = – 300000 m/s; Series-4 : J = 2, V_{Di} = – 100000 m/s; Series-5 : J = 2, V_{Di} = – 200000 m/s; Series-6 : J = 2, V_{Di} = – 300000 m/s; Series-7 : J = 4, V_{Di} = – 100000 m/s; Series-8 : J = 4, V_{Di} = – 200000 m/s; Series-9 : J = 4, V_{Di} = – 300000 m/s].

frequency (ω/Ω_i) for different valus of ion beam velocity (V_{Di}) at constant electron beam velocity and distribution index 'J' for the first harmonic of the ion cyclotron wave. It is assumed that the ion beam is directed from the ionosphere towards the magnetotail and therefore, the ion beam velocity is negative. It is observed that the effect of increasing ion beam velocity is to reduce the growth rate that may be due to the shifting of resonance condition. The effect of higher distribution index is to enhance the growth rate. Thus, the mirror like structure of the magnetosphere with a steep distribution index may be unstable for the EIC wave emission. It is also observed that the growth rate decreases with the increasing values of ω/Ω_i which may be due to the shifting of the resonance condition. Hence, the wave energy is being transferred to the particles.

Figure 2 shows the variation of transverse resonant energy ($Wr_\perp$), in joules, with the wave frequency (ω/Ω_i) of the wave for different values of V_{Di} and 'J' at constant V_{De} for the first harmonic of the ion cyclotron wave. It is observed that the effect of increasing V_{Di} is to increase the transverse resonant energy. Thus, the perpendicular acceleration of charged particles is possible through the ion cyclotron wave at the cost of ion beam energy. The effect of increasing distribution index is to decrease the transverse resonant energy. Thus, the steep loss-cone

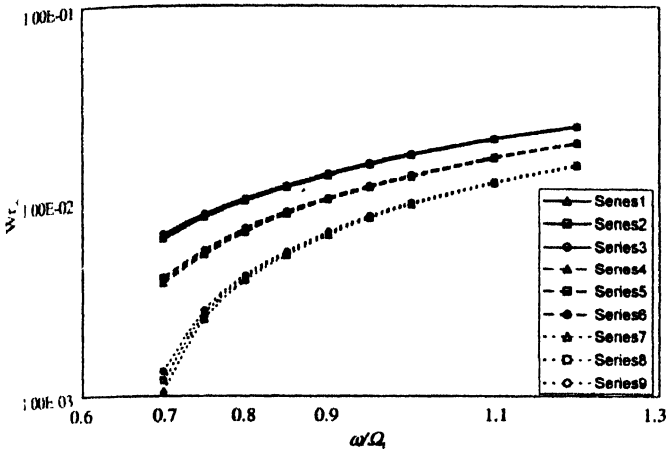

Figure 2. Variation of $Wr_\perp$ with ω/Ω_i for different values of V_{Di} and J. [Series-1 : $J = 0$, $V_{Di} = -100000$ m/s; Series-2 : $J = 0$, $V_{Di} = -200000$ m/s; Series-3 : $J = 0$, $V_{Di} = -300000$ m/s; Series-4 : $J = 2$, $V_{Di} = -100000$ m/s; Series-5 : $J = 2$, $V_{Di} = -200000$ m/s; Series-6 : $J = 2$, $V_{Di} = -300000$ m/s; Series-7 : $J = 4$, $V_{Di} = -100000$ m/s; Series-8 : $J = 4$, $V_{Di} = -200000$ m/s; Series-9 : $J = 4$, $V_{Di} = -300000$ m/s].

distribution of the magnetosphere stabilizes the transverse resonant energy. It is also observed that $Wr_\perp$ increases with the increasing values of ω/Ω_i. The increase in heating of the particles by the ion beam is supported by the decrease in growth rate, as the wave energy is being transferred to the particles by the resonance interaction process.

Figure 3 depicts the variation of parallel resonant energy ($Wr_\parallel$) in joules, with wave frequency (ω/Ω_i) for different values of V_{Di} and for the increasing values of the distribution index at constant V_{De} for the first harmonic of the ion cyclotron wave. Here, it is observed that $Wr_\parallel$ decreases when $\omega < \Omega_i$, becomes minimum when $\Omega_i \sim \omega$, and for $\omega > \Omega_i$, $Wr_\parallel$ increases *i.e.* for $\omega < \Omega_i$ the parallel energy is being transferred for perpendicular energisation and the wave energy is being transferred to the parallel resonating particles only for $\omega > \Omega_i$. For $\omega > \Omega_i$, effect of V_{Di} is to increase the parallel resonant energy. Thus, the heating of resonant ions parallel to magnetic field may be enhanced by the ion beam. The effect of increasing values of the distribution index is to decrease the parallel resonant energy. Thus, the steep loss-cone distribution of the magnetosphere stabilizes the parallel resonant energy of the EIC wave.

The effect of electron beam velocity (V_{De}) at constant V_{Di} and the distribution index on the growth rate and the energy transferred for the first harmonic of the wave, is depicted in Figures 4, 5 and 6. Figure 4 shows the variation of growth rate with wave frequency for different values of V_{De} and J. It is observed that the growth rate increases with the electron beam velocity which may be due to the shifting of resonance condition. Since the EIC waves have a finite wave number component along the magnetic field, the electron beams streaming along the magnetic field may destabilize them. However, very high electron beam velocity leads to saturation of instability and the growth rate is slightly affected by the increase of the beam velocity. This may be due to the fact that the beam velocity slightly above the phase velocity of the wave, is most effective in its interaction with the wave in the resonance condition. The effect of J is also to increase

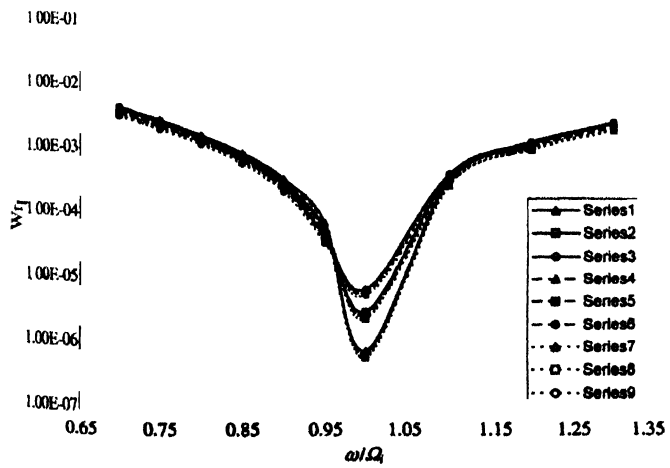

Figure 3. Variation of $Wr_\parallel$ with ω/Ω_i for different values of V_{Di} and J. [Series-1 : $J = 0$, $V_{Di} = -100000$ m/s; Series-2 : $J = 0$, $V_{Di} = -200000$ m/s; Series-3 : $J = 0$, $V_{Di} = -300000$ m/s; Series-4 : $J = 2$, $V_{Di} = -100000$ m/s; Series-5 : $J = 2$, $V_{Di} = -200000$ m/s; Series-6 : $J = 2$, $V_{Di} = -300000$ m/s; Series-7 : $J = 4$, $V_{Di} = -100000$ m/s; Series-8 : $J = 4$, $V_{Di} = -200000$ m/s; Series-9 : $J = 4$, $V_{Di} = -300000$ m/s].

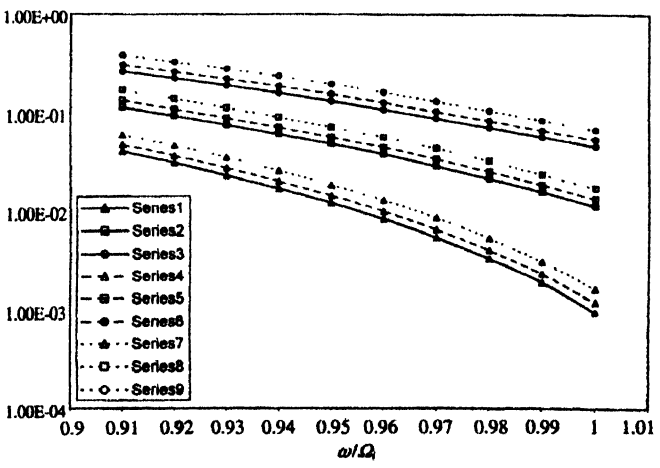

Figure 4. Variation of γ/ω with ω/Ω_i for different values of V_{De} and J. [Series-1 : $J = 0$, $V_{De} = 1000000$ m/s; Series-2 : $J = 0$, $V_{De} = 2000000$ m/s; Series-3 : $J = 0$, $V_{De} = 3000000$ m/s; Series-4 : $J = 2$, $V_{De} = 1000000$ m/s; Series-5 : $J = 2$, $V_{De} = 2000000$ m/s; Series-6 : $J = 2$, $V_{De} = 3000000$ m/s; Series-7 : $J = 4$, $V_{De} = 1000000$ m/s; Series-8 : $J = 4$, $V_{De} = 2000000$ m/s; Series-9 : $J = 4$, $V_{De} = 3000000$ m/s].

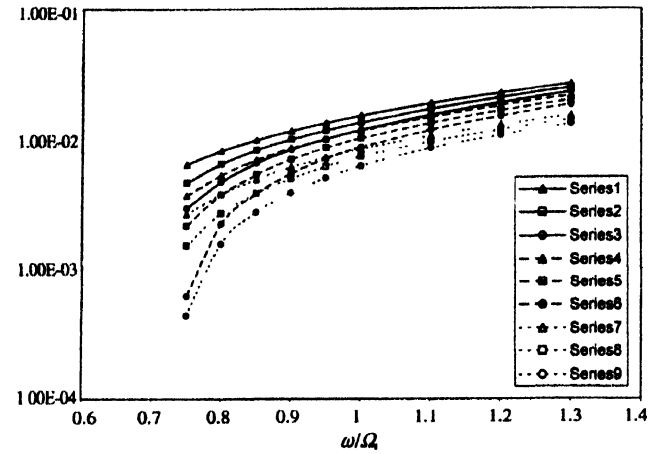

Figure 5. Variation of $Wr_\perp$ with ω/Ω_i for different values of V_{De} and J. [Series-1 : $J = 0$, $V_{De} = 1000000$ m/s; Series-2 : $J = 0$, $V_{De} = 2000000$ m/s; Series-3 : $J = 0$, $V_{De} = 3000000$ m/s; Series-4 : $J = 2$, $V_{De} = 1000000$ m/s; Series-5 : $J = 2$, $V_{De} = 2000000$ m/s; Series-6 : $J = 2$, $V_{De} = 3000000$ m/s; Series-7 : $J = 4$, $V_{De} = 1000000$ m/s; Series-8 : $J = 4$, $V_{De} = 2000000$ m/s; Series-9 : $J = 4$, $V_{De} = 3000000$ m/s].

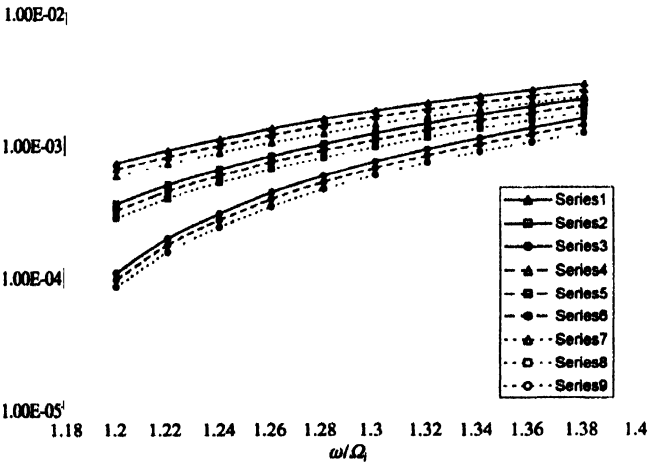

Figure 6. Variation of $Wr_\parallel$ with ω/Ω_i for different values of V_{De} and J. [Series-1 : $J = 0$, $V_{De} = 1000000$ m/s; Series-2 : $J = 0$, $V_{De} = 2000000$ m/s; Series-3 : $J = 0$, $V_{De} = 3000000$ m/s; Series-4 : $J = 2$, $V_{De} = 1000000$ m/s; Series-5 : $J = 2$, $V_{De} = 2000000$ m/s; Series-6 : $J = 2$, $V_{De} = 3000000$ m/s; Series-7 : $J = 4$, $V_{De} = 1000000$ m/s; Series-8 : $J = 4$, $V_{De} = 2000000$ m/s; Series-9 : $J = 4$, $V_{De} = 3000000$ m/s].

the growth rate as is discussed earlier. Figure 5 shows the variation of $Wr_\perp$ (in joules) with wave frequency for different electron beam velocity (V_{De}) at constant V_{Di} and J. The effect of V_{De} is to reduce $Wr_\perp$ that may be due to the ion cyclotron interaction. $Wr_\perp$ decreases with increasing J as discussed earlier. From Figure 6, it is observed that V_{De} shows reducing effect on $Wr_\parallel$ (in joules) which decreases with J also, as discussed earlier. The reduction is transverse and parallel energy by the electron beam velocity (V_{De}) is supported by the increase in the growth rate, as the particle energy is being transferred to the wave by the resonance interaction processes. Thus, the wave may be generated by extracting energy from the resonant particles in the presence of the electron beam.

Thus, the electron beam acts as a source of free energy for the EIC waves. It modifies the wave-particle resonance condition and leads to weakening of Landau damping effects and enhances growth rate. The wave extracts the electron beam energy through its electric field directed parallel to the magnetic field. However, the effect of the ion beam is to reduce the growth rate of the wave but to increase the transverse acceleration of the ions. The results are consistent with the findings of Singh *et al* [22], Sugawa and Utsunomiya [23] and Hwang and Okuda [24] and rocket and satellite observations.

The effect of distribution index is also to increase the growth rate of the wave but to decrease the transverse acceleration of the ions. The destabilizing effects due to the steep loss-cone on different instabilities have also been reported by various workers [19,25]. The steep loss-cone structures are analogous to mirror-like devices with higher mirror ratio that may accelerate the charge particles moving perpendicular to the magnetic field. Thus, more energetic particles may be available to provide energy to the wave by wave-particle interaction.

EIC waves are often detected in the inverted-V structures of the auroral acceleration region [7,8]. Recently, a FAST satellite has observed intense EIC wave turbulences upto 1000 Hz in association with ion and electron beam in the upward current auroral region [11]. Coherent ion cyclotron waves with amplitude upto 50 mV/m in association with upgoing ~1 keV ion beam and downgoing ~ 800 eV electron beam, have also been observed recently by a Polar satellite in the auroral zone [10]. Local ion cyclotron with frequency ~100 Hz in association with downgoing electrons ($\lesssim$ 100 eV) and upflowing ion beams have also been observed by the same satellite in an upward field aligned current region. The same Polar satellite has also observed local hydrogen ion cyclotron wave of amplitude 500 mV/m in association with upward 1 keV accelerated ion beam and downward 5 keV accelerated electron beam at lower altitudes. EIC waves of frequency ~105 Hz in association with upgoing ion beam of 2 keV energy and downcoming electron beam of 1 keV energy have also been observed in the magnetosphere by the satellite [10].

The results obtained may be useful to study the electrodynamics of the auroral acceleration region. The EIC turbulence has been considered as a possible source

of anomalous resistivity. When the instability occurs, the field energy grows exponentially; therefore, the loss of kinetic energy of electrons is also exponential and the current carried by these electrons is suddenly disrupted [3]. Such instabilities can produce anomalous resistivity. Recently, transversely accelerated ions and their association with the ion cyclotron waves at altitudes upto few thousand kilometers has been reported by the analysis of the Freja satellite data [5]. The anomalous resistivity produced by the EIC wave leads to an anomalous version of the Joule heating effect in the topside ionosphere or lower magnetosphere and transfer of energy occurs from the EICI to ion thermal motion. Owing to this heating in this cyclotron motion, the total energy of the ions rapidly increases and this becomes subject to the gradient $\boldsymbol{B}$ or mirror force by means of which they are ejected for the perpendicular energisation. The process of perpendicular ion energisation gives rise to ion distribution, which are known as transverse acceleration of ions (TAI). The ion beam enhances the heating rate of TAI whereas the electron beam and the steep loss-cone controls the heating rate of TAI through the EICI in the presence of ion and electron beams in the auroral acceleration region and transfers this energy to the wave *via* inverse Landau damping. Recently, a Polar satellite has observed EIC waves in the auroral acceleration region containing ion conics [10]. EIC wave heating is one of the major candidates for ion conic formation. The ion conic distributions have been interpreted as resulting from perpendicular heating of ions at low altitudes followed by parallel upward adiabatic motion due to the magnetic mirror force. The turbulent resistivity produced by EIC instability allows parallel electric field to develop along the parallel field lines. This parallel electric field may lead to upflowing ion beam and downcoming electron beam which may generate the EIC wave.

Recent observations by the Viking [13] and the Freja satellite [5] indicate that EIC waves and the ion and electron beams in the plasma sheet boundary layer give rise to broad band extremely low frequency (BB-ELF) instabilities [14]. BB-ELF emissions are extremely low frequency electric and magnetic field fluctuations observed [5] in the range 1 Hz–3 kHz. These emissions have been detected within regions of auroral inverted-V electron precipitation at a few 1000 km altitude as well as in the magnetospheric tail at several earth-radii, in the magnetospheric day side cusp/cleft and in the topside auroral ionosphere from altitudes of a few 100 km to a couple of 1000 km. Gyro resonant heating by these waves around the gyro-frequency also gives rise to intense events of transverse acceleration of ions [5]. At least at altitudes from 1000 km up to several 1000 km, most of the ion energisation is associated with BB-ELF waves.

The EIC turbulence plays an important role in the loss-cone current-potential relationship. It leads to spatial variations in the double layer potential and thereby produces thin auroral arcs embedded in inverted-V precipitation [7,8]. It has also been suggested that the loss-cone effect can enhance the anomalous resistivity for a given turbulence level. Since the steep loss-cone distribution in the presence of EIC wave and the electron beam enhances the growth rate, the anomalous resistivity and transport resulting from this instability is likely to play crucial role in the auroral acceleration region. The equilibrium dipolar magnetic field of the earth is curved in the meridinal plane and introduces loss-cone effects in the particle distribution function [19]. Thus, the behaviour studied for the EIC wave may be of importance in the electrostatic emission in the auroral acceleration region.

In most of the theoretical work, the velocity distribution functions have been assumed to be ideal Maxwellian [2,16–18], although most turbulent heating experiment have been done in mirror like devices which in general allow non-Maxwellian, particularly loss-cone distribution. The theory developed in the present work may be applicable to such hot particle mirror experiments. Single particle theory may be able to explain some of the plasma phenomenon that other theories may not.

Acknowledgment

One of the authors (MST) is thankful to Indian Space Research Organization (ISRO) for the financial assistance.

References

[1] J M Kindel and C F Kennel *J. Geophys. Res.* **76** 3055 (1971)

[2] G Ganguli *Phys. Plasmas* **4** 1544 (1997)

[3] C T Dum and T H Dupree *Phys. Fluids* **13** 2064 (1970)

[4] P M Kintner, W Scales, G Vago, R Arnoldy, G Garbe and T Moore *Geophys. Res. Lett.* **16** 739 (1989)

[5] J E Wahlund, A I Eriksson, B Holback, M H Boehm, J Bonnell, P M Kintner, C E Seyler, J H Clemmons, L Elaisson, D J Knudsen, P Norquist and L J Zanetti *J. Geophys. Res.* **103** 4343 (1998)

[6] V V Gavrishchaka, S B Ganguli and G I Ganguli *Geophys. Res.* **104** 12683 (1999)

[7] F S Mozer, C W Carlson, M K Hudson, R B Torbert, B Parady, J Yatteau and M C Kelley *Phys. Rev. Lett.* **382** 2599 (1977)

[8] F S Mozer, C A Cattell, M K Hudson, R L Lysak, M Temerin and R B Torbert *Space Sci. Rev.* **27** 155 (1980)

[9] S Basu, E MacKenzie, P F Fourgere, W R Coley, N C Maynard, J D Winningham, M Sagiura, W B Hanson and W R Hoegy *J. Geophys. Res.* **93** 115 (1988)

[10] F S Mozer, R Ergun, M Temerin, C Cattell, J Donsbeck and J Wygant *Phys. Rev. Lett.* **79** 1281 (1997)

[11] V V Gavrishchaka, G I Ganguli, W A Scales, S P Slinker, C C Chatson, J P McFadden, R E Ergun and C W Carlson *Phys. Rev. Lett.* **85** 4285 (2000)

[12] B H Mauk and L J Zenetti *Rev. Geophys.* **25** 541 (1987)

[13] R Lundin, G Haerendel, M Bohem and B Holback *Geophys. Res. Lett.* **21** 1903 (1994)

[14] S V Singh and G S Lakhina *Planet. Space Sci.* **49** 107 (2001)

[15] F S Mozer and A Hull *J. Geophys. Res.* **106** 5763 (2001)

[16] R Bharuthram, P Singh, M Rosenberg and V W Chow *Phys Scr.* **T75** 223 (1998)

[17] V V Gavrishchaka, M E Koepke and G I Ganguli *J. Goephys. Res* **102** 11653 (1997)

[18] V E Zakhrov and C V Meister *Astronomische Nachrichten* **320** 425 (1999)

[19] R Gaelzer, R S Schneider and L F Ziebell *Phys. Rev. E* **55** 5859 (1997)

[20] J M Dawson *Phys. Fluids* **4** 869 (1961)

[21] Y Terashima *Prog. Theor. Phys.* **37** 661 (1967)

[22] N Singh, J R Conard and R W Schunk *J. Geophys. Res.* **90** 12219 (1985)

[23] M Sugawa and S Utsunomiya *Plasma Phys. Contr. Fusion* **31** 57 (1989)

[24] Y S Hwang and H Okuda *J. Geophys. Res.* **94** 10103 (1989)

[25] A K Dwivedi, P Varma and M S Tiwari *Planet. Space Sci.* **49** 993 (2001)